Vietnam Journal of Catalysis and Adsorption
Tạp chí xúc tác và hấp phụ Việt Nam

https://jca.edu.vn

Synthesis of CQDs/MIL-101(Cr) photocatalytic nanocomposite for degradation of RR-195

Nguyen Thi Hong Van[1], Nguyen Thi Tra[2], Pham Xuan Nui[2*]

[1]*Institute of Environment, Vietnam Maritime University, 484 Lach tray street, Le Chan, Hai Phong, VIETNAM*
[2]*Department of Chemical Engineering, Hanoi University of Mining and Geology, 18 Pho Vien, Duc Thang, Bac Tu Liem, Hanoi, VIETNAM*
**Email:phamxuannui@humg.edu.vn*

ARTICLE INFO

Received: 10/02/2024
Accepted: 15/3/2024
Published: 30/3/2024

Keywords:
CQDs, UiO-66, RR-195 degradation, photocatalyst, nanocomposite

ABSTRACT

CQDs, characteristically quasispheroidal carbon nanoparticles composed of amorphous to crystalline carbon base, is a prospective semiconductor quantum dots owing to its excellent optical absorptivity, chemical stability, nontoxicity, and facile synthesis. In this study, we demonstrated the impregnation method to integrate CQDs, formed from chitosan with MIL-101(Cr) from terephthalic acid recycled by PET waste to synthesize CQDs/MIL-101(Cr) nanocomposite. After the hybridization of CQDs with MIL-101(Cr), the band gap energy of the 50% CQDs/MIL-101(Cr) has the lowest Eg (1.98 eV), allowing the demonstration of photocatalytic activity under high visible light. This material was tested in the photodegradation RR-195 dye and compared with the pristine components. The highest RR-195 degradation efficiency was recorded when using catalyst mass: 50 mg of 50% CQDs/MIL-101(Cr) catalyst samples, dye concentration: 50 ppm after 4 h under xenon lamp 300w was 96%. These results could promote a new material as a new semiconductor that can be used to protect water from further pollution.

1. Introduction

Recently, carbon quantum dots (CQDs), a new class of carbon nanoparticles, have attracted much attention as a prospective semiconductor quantum dot owing to its excellent optical absorptivity, chemical stability, nontoxicity, and facile synthesis. CQDs are characteristically quasispheroidal carbon nanoparticles composed of amorphous to crystalline carbon bases. It is primarily made up of sp^2-graphitic carbon (or) graphene and graphene oxide sheets combined through the insertion of sp^3-hybridized carbon that exhibits fluorescence properties [1]. Moreover, physicochemical properties of CQDs, such as the solubility of CQDs in water and surface functionalization, ... can be easily modified due to the presence of various functional groups on their surfaces such as hydroxyl, carboxyl, ester, ether or amino with inorganic, organic polymeric or biological species. For example, CQDs prepared from chitosan is not only rich in C atoms but it also contains numerous -OH and-NH_2 groups as well as amino glucose and N-acetylamino glucosemers linked by glycosidic bonds, applied widely in medicine and pharmacy as three-dimensional scaffold in wound dressings or elements of controlled drug delivery and release systems [2]. Especially, their photoluminescent properties are not only size- and shape-dependent. As edge shapes, surface ligands and defects also play significant roles in determining their final characteristics as well as their photoluminescence depending on excitation wavelength (when CQDs are excited by UV to VIS, their emission wavelengths range from the UV to the near-IR region) [2]. Therefore, CQDs, potential replacement for the toxic metal-based quantum dots, are being used in various fields of applications, such as bioimaging, medical diagnosis, biosensing, chemical sensing, photocatalysis, and photovoltaic devices [1].

https://doi.org/10.62239/jca.2024.018

Working as a cocatalyst, CQDs can play a versatile role such as an electron receptor, a photosensitizer, and/or a spectral converter, depending on the specific photocatalytic system. Therefore, CQDs have been intensively applied to combine with some inorganic photocatalysts and their application as a localized electron acceptor inside a MOF particle are to expand photosensitizers under long wavelength light irradiation of photocatalysts [3].Metal–organic frameworks (MOFs) are a class of porous crystalline materials assembled from metal ions (or clusters) and organic linkers, featuring well-defined pore structures, high surface area and opened channels. When employed as photocatalysts, MOF materials can offer tremendous and dispersive active sites that are accessible to substrates/products via the opened channels. Furthermore, each active site (e.g., metal-oxo cluster) in MOFs can be regarded as a single quantum dot, serving as a light absorber, a charge generator, and a catalytic site like a small semiconductor. Moreover, the organic linkers in MOFs can work as antennas to absorb extra ultraviolet (UV) light and transfer energy to the active sites via the ligand-to-metal charge transfer (LMCT) process [3]. Recently, some researchers reported to generate CQDs inside typical MOF photocatalysts to make prominent materials. Such as Rongbin Lin et al. embedded the CQDs into MIL-53(Fe) particles, which exhibit giant activity enhancement toward Cr(VI) reduction [3], while Xiaoyan Wei proposed the photocatalytic activity of CQDs/ZIF-8 composite under visible light was tested by removing gaseous NO in continuous air flow [4]. In recent research, we are developing some MOF materials that use BDC recycling from PET waste (which has led to serious environmental problems because of their poor biodegradability) as a key ingredient, including chromium (III)-carboxylate MOFs (Cr-MOFs). MIL-101(Cr), it has been explored as a potential candidate for photocatalysis due to its high moisture stability, good thermal stability, large pore volume and surface area, as well as numerous unsaturated chromium sites. [5]

From this inspiration and above overview study, we proposed the use of terephthalic acid produced from recycled plastic bottles and chitosan as cheaper sources for the synthesis of MIL-101(Cr) and CQDs, respectively. After that, these pristine materials were integrated into nanocomposite CQDs/MIL-101(Cr) which is the new structure of material for enhancing of photocatalyst ability. CQDs/MIL-101(Cr) was tested in the photodegradation of RR 195 and was compared with the pristine components.

2. Experiments and research methods

Materials

Chromium (III) nitrate nonahydrate ($Cr(NO_3)_3.9H_2O$, 99%), chitosan (deacetylation degree $C_6H_{11}NO_4$ 82.5%), acid terephthalic (H_2BDC 99.8%), sodium hydroxide (NaOH, 98%), sulfuric acid (H_2SO_4, 98%), hydrofluoric acid (HF), acid acetic (CH_3COOH 99%), hydrogen peroxide 30% (H_2O_2), dimethylformamide (DMF, 99.8%), ethylene glycol (EG, 99%), methanol (CH_3OH), ethanol (C_2H_5OH), deionized water and TPA was recovered from polyethylene terephthalate (PET) according to our previous study [6].

Synthesis of MIL-101(Cr)

The components 5.6 g of $Cr(NO_3)_3.9H_2O$, 1.6 g of TPA and 0.3 mL HF and 45 mL of deionized water. The solution will be mixed by ultra-sonification in 15 min, then transferred to the Teflon-lined stainless-steel autoclave and heated up to 220°C in the oven. After 8h, the mixture was cooled down naturally, the product after hydrothermal was a dark blue crystalline solid, MIL-101 (Cr). To purify the solid, the solid was washed in dimethyl formide (DMF) at 100℃ for 3 h, ethanol at 80℃ for 24, then ammonium fluoride (NH_4F) solution at 70℃ for 24 h. Finally, the MIL-101(Cr) is dried once at 80°C in 12h.

Synthesis of CQDs

The CQDs were prepared by the hydrothermal method using chitosan solution as a reaction precursor according to the method reported by Yang with some modifications. The typical synthesis is described as follows: firstly, 0.5 g of chitosan was added to 100 mL of 1% acetic acid solution and dissolved at room temperature using ultrasonic technique, and then the prepared chitosan solution was filtered to remove the insoluble substance. Secondly, the solution was placed in an autoclave (50 mL) and heated at 180°C for 12 h. Thirdly, when cooled down to room temperature, the brownish black solution was filtered. Next, the solution was centrifuged at 10000 rpm for 15 min to remove all deposits and yield a canary yellow CQD aqueous solution, and then the as-prepared CQDs were stored in a refrigerator at 4°C for future use. The final CQDs were denoted as CHI-12, where 12 referred to the carbonization time.

Synthesis of CQD/MIL-101(Cr)

The CQDs/MIL-101(Cr) photocatalyst was prepared by an impregnation method. CQDs were immobilized onto the surface of MIL-101(Cr). The synthesized 0.1g of MIL-

https://doi.org/10.62239/jca.2024.018

101(Cr) was dispersed in 20 mL of ethanol, then 5 mL of CQDs solution was introduced to the suspension dropwise, and the mixture was sonicated in an ice bath for 30 min. Next, the suspension was magnetically stirred at room temperature for 24 h to achieve adsorption equilibrium. The final product was obtained by centrifugation and purged with deionized H_2O three times, desiccated naturally in the fume hood.

Characterisation

The crystal lattice structure of the synthesized samples was determined by X-ray powder diffraction (XRD) using a D8 ADVANCE system (Cu Ka1 copper radiation, λ = 0.154 nm, 3° min-1 scanning speed, Bruker, Germany). The UV-vis diffuse reflectance (DRS-UV) and photoluminescence (PL) spectra were performed with the UV-2600 spectrophotometer (Shimadzu) and the Cary Eclipse fluorescence spectrophotometer (Varian), respectively. Surface morphology was observed by a scanning electron microscope (S-4800, Hitachi). The Fourier transform infrared spectra (FT-IR) were measured with an FT-IR Affinity-1S (SHIMADZU).

Photocatalytic experiments

The photocatalytic activity of CQDs/MIL-101(Cr) materials was evaluated by decomposition of Reactive Red 195 (RR 195) dye in water using simulated sunlight. In the experiment, 50 mg of the catalyst was dispersed in RR 195 solution (30 mL, 50 ppm). Before simulated sunlight irradiation, the mixture was magnetically stirred for 60 min to reach adsorption-desorption equilibrium. After 1 h, the mixture was exposed to simulated sunlight, at fixed intervals, 5 mL of the solution sample was removed, centrifuged to remove solids. The solution fraction was analyzed using a UV-Vis 2450 spectrophotometer at a maximum absorption peak of 541 nm. The initial solution concentration is called C_o, the solution concentration after each time interval is C_t. The decomposition efficiency is calculated by the formula:

$$\%H = \frac{C_o - C_t}{C_o}.100$$

3. Results and Discussion

Characterisations of materials

From Figure 1(A) on chitosan (a) and CQDs (b) illuminated by natural light, chitosan after being dissolved in 1% acetic acid solution and after hydrothermal to CQDs, the growth of their fluorescence emission cannot be seen. To know if chitosan and CQDs have fluorescence? For visual observation of their fluorescence, chitosan and CQDs were illuminated by a UV lamp with 365 nm light. In Figure 1(B) chitosan solution(c) irradiated under a UV lamp shows no fluorescence emission. While CQDs (d) solution shows blue light under a UV lamp clearly, showed that CQDs have fluorescence emission and can also be considered to have synthesized CQDs.

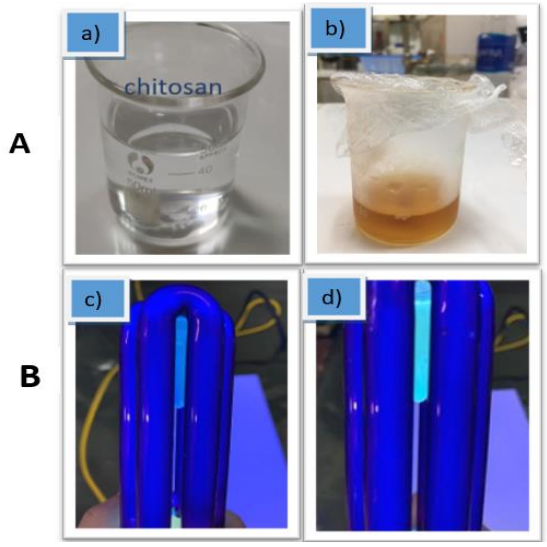

Fig 1: From left to right are photographs of chitosan (A): a), CQDs b) illuminated by natural light. (B): From left to right are photographs of chitosan c), CQDs d) illuminated by an UV lamp with light 365nm

Figure 2 (a) shows that XRD patterns of the typical peak at around 21 ($2\boldsymbol{\theta}$) corresponded to the diffraction peaks of (240), (002) of the carbon material. Besides that, patterns of MIL-101(Cr) were recorded at $2\boldsymbol{\theta}$ = 3.29°, 4.08°, 5.26°, 6.02°, 8.54°, and 9.18°, corresponding to the featured diffraction peaks of the calculated crystallographic planes of (311), (400), (511), (531), (822), and (911) in MIL-101(Cr), respectively [7]. The presence of prominent peaks of MIL-101(Cr) and CQDs are observed and remain although the peak intensities are gradually weakened. It could be due to the CQDs loaded onto the surface and into pore of MIL-101(Cr) structure.

FT-IR spectroscopy was performed to detect chemical compositions and sample bonding. For samples of MIL-101(Cr) and CQD/MIL-101(Cr), FT-IR patterns are observed in Figure 2 (b). The peaks between 580 cm^{-1} for MIL-101(Cr) can be attributed to the vibrations of Cr-O stretching and successfully represented the [10] connection among the metal Cr^{3+} and (-COO)-group of TPA [8] and the peaks in the range of 1500–1700 cm^{-1}

https://doi.org/10.62239/jca.2024.018

correspond to the vibrations of C-O and asymmetric stretching vibration of COO-, respectively. The peaks of 1512cm^{-1} and 1393 cm^{-1} bands corresponded to C=C vibration. In addition, the peaks at 1160, 1017, 885 and 750 cm^{-1} performed characteristic of aromatic ring. In the FT-IR spectrum of the CQDs, it is found that the strong absorption in the range of 3200–3400 cm^{-1} corresponds to the stretching vibration of –OH, which proves that the surface of the CQDs contains -OH [9] and the characteristic peaks for C–O, –COOH and –OH are observed at the same wavelength in CQDs@MIL-101(Cr).

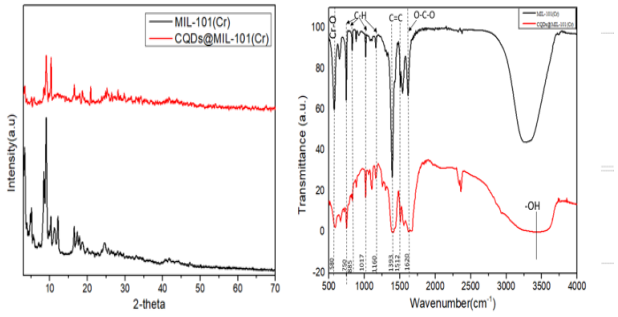

Fig 2: a) XRD patterns of MIL-101(Cr) and CQD/MIL-101(Cr); b) FT-IR spectra of MIL-101(Cr) and CQDs/MIL-101(Cr)

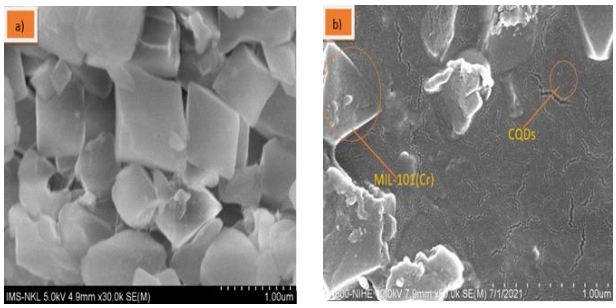

Fig 3: Images SEM of a) MIL-101(Cr) and b) CQDs/MIL-101(Cr)

The electron microscopy (SEM) image shown in Figure 3 (a) shows that MIL-101(Cr) has a uniform shape and structure, the morphology of MIL-101(Cr) consists of octahedral crystals with a surface smooth. The presence of CQDs after being mounted on MIL-101(Cr) in Figure 3 (b) shows that CQDs are evenly dispersed on the surface of MIL-101(Cr), the particle size of CQDs is 10 nm.

Optical properties

The band-gap energies of the samples could be estimated by Tauc's plots: $(\alpha h\nu) = A(h\nu - Eg)^{n/2}$, where α, h, ν, A, and Eg are indicative to the absorption coefficient, Planck's constant, light frequency, constant value, and band-gap energy, and n is 1 to 4 for a direct and indirect band-gap semiconductor, respectively.
While Fig. 4 shows the diffused reflectance spectra and band gap of the MIL-101(Cr) and CQDs/MIL-101(Cr) composites.

As depicted in Fig. 4(a), it could be seen that MIL-101(Cr) exhibits visible light absorption the absorption edge near 380 nm, other absorption bands in the extended region to 700 nm can be detected and represented d-d transition band of Cr^{3+}, whereas the absorption bands of the 25%, 50%, and 75% CQDs/MIL-101(Cr) composites also tend to a visible light wavelength from 380 nm to 700nm.

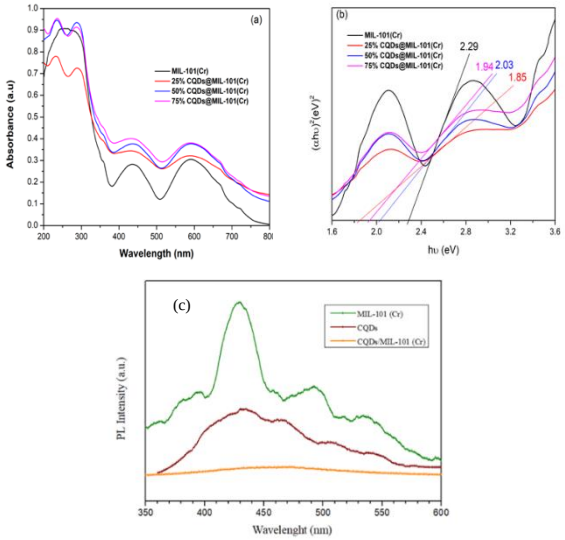

Fig 4: a) and b) DRS and band gap estimation of MIL-101(Cr) and CQDs/Mil-101(Cr); c) Fluorescence emission spectra (PL) of CQDs, MIL-101(Cr) and CQDs@MIL-101(Cr)

The plot of $(\alpha h\nu)^{1/2}$ or $(F(R)h\nu)^{1/2}$ versus hν is exhibited for MIL-101(Cr) and the composites as shown in Fig. 4(b). Herein, the band gaps of MIL-101(Cr) are estimated to be about 2.18eV, respectively. In addition, the band gap energy of 25%, 50%, 75% CQDs/MIL-101(Cr) were calculated to 2.02, 1.98, 2.06 eV, respectively. Sample 50% CQDs/MIL-101(Cr) has the lowest Eg (1.98 eV) demonstrating that the ability of this material to absorb visible light is better than the remaining samples. To clarify the separation and recombination of photogenerated electron and hole pairs, fluorescence emission spectra (PL) of synthesized materials were shown in Figure 4 c). As shown in Figure 4 c), the PL emission peak was recorded at 429 nm with an excitation wavelength of 360 nm at room temperature. The PL emission peak of MIL-101(Cr) is at 429 nm and has the highest emission intensity, representing the fast recombination of the photogenerated electron-hole

https://doi.org/10.62239/jca.2024.018

pairs. The CQDs/MIL-101(Cr) of composites has the lowest emission peak and almost no comparison among CQDs and MIL-101(Cr). This result implied that the CQDs/MIL-101(Cr) posed as the highest suppression of photogenerated electron-hole recombination rate.

Photocatalytic activity

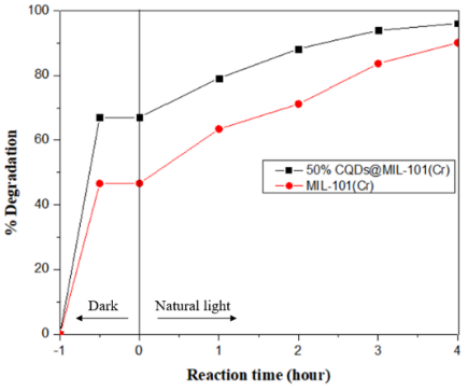

Fig 5: Effect of photocatalysts on the degradation of dye RR 195

The photodegradation performance of the catalysts MIL-101(Cr) and CQDs/MIL-101(Cr) were studied through the degradation of dye RR 195, under reaction conditions as catalyst weight: 50 mg, concentration RR 195: 50 ppm, reaction time: 4h, illuminated by a 300 W Xenon lamp. From Figure 5, compared with CQDs/MIL-101(Cr), the degradation efficiency of RR 195 of the material after 4 hours is 96.52%, while the degradation efficiency of RR 195 after 4 hours of MIL-101(Cr) is 90.1%. This can be explained that the material CQDs/MIL-101(Cr) can perform better under the visible light region, leading to the excitation to generate many photogenerated electron-hole pairs, on the other hand, the advantages of surface and capillary structure make the decomposition of RR 195 under simulated sunlight highly efficient. The reactions were performed after 4 h of illumination by a 300W Xenon lamp with 20 mL of 70 ppm RR 195 dye and a pH = 6.5 for experiments in Figure 6 a,b,c,d. To investigate the influence of the catalyst dosage on the degradation of RR 195, the experiment was carried out under the following conditions: catalyst weight was 25, 50, and 100 mg, dye concentration: 50 ppm, reaction time: 4 h, illuminated by a 300 W Xenon lamp.

The results obtained in Figure 6 a) show that the highest photocatalytic efficiency reaches 96 % after 4 h corresponding to 50 mg of catalyst and then the efficiency tends to decrease when increasing the amount of catalyst to 100 mg. With a large amount of catalyst, the formation of active sites will increase, however, when the amount of catalyst is too high, it will cause interactions between the surface layers of the material, reducing the formation of electron-hole photogenerated layers internally resulting in a reduced photocatalytic efficiency [11]. The reaction conditions are as follows: 30 mL of 50ppm RR 195 dye, the catalyst weight is 500 mg, illuminated by a 300 W Xenon lamp conditions, pH=6.5. As Figure 6 b), after 4 hours illuminated by a 300 W Xenon lamp, about 99% RR 195 decomposed when H_2O_2, while about 97% RR 195 decomposed when not using H_2O_2. Therefore, the photocatalytic activity of CQDs/MIL-101(Cr) materials did not change much in the presence and absence of H_2O_2. This can be explained by the doping of the oxygen atom which greatly improved the separation efficiency of photogenerated electron and hole pairs on the catalyst. From that showed the use of H_2O_2 is not necessary in the process of decomposition of dye RR 195.

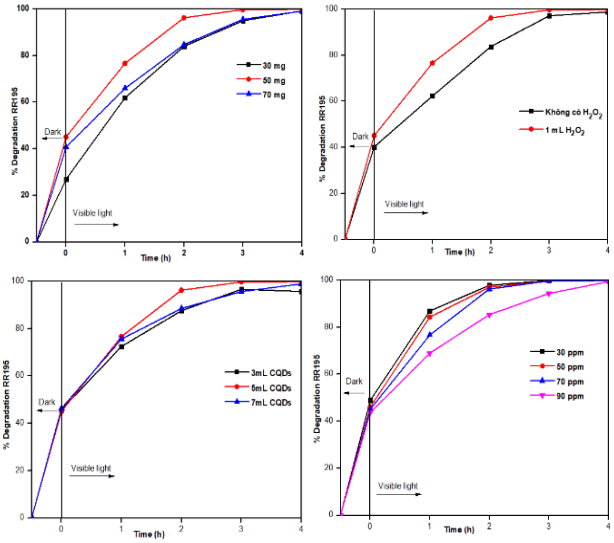

Fig 6: Photodegradation of RR195 using (a) various amounts of CQDs/MIL-101(Cr); (b) photocatalyst CQDs/MIL-101(Cr) without H_2O_2 and with 1 mL H_2O_2; (c) various concentrations of CQDs/MIL-101(Cr); (d) various concentration of RR 195 to the photocatalytic ability of CQDs/MIL-101(Cr)

The influence of the content of CQDs/MIL-101(Cr) on the ability to degrade dye RR 195 was carried out under the following conditions: catalyst weight: 50 mg, RR 195 concentration: 50 ppm, time reaction time: 4h, pH=6.5. Figure 6 c) shows that the content of CQDs has a great influence on the photocatalytic performance of the material. The material 50% CQDs/MIL-101(Cr) has the highest photocatalytic activity, can decompose RR 195 to 96.52% after 4 hours of light. While the 75% sample CQDs/MIL-101(Cr) has the degradation efficiency of RR 195 reaching 90.03% after 4 hours of light. This may be due to excess CQDs clumping together, preventing

https://doi.org/10.62239/jca.2024.018

photogenesis of electron-hole formation. Experiments were carried out at the following reaction conditions: mass 50 % CQDs/MIL-101(Cr): 50 mg, dye concentration: 30-90 ppm, reaction time: 4h, illuminated by a 300 W Xenon lamp. From Figure 6 d), it was observed that when the dye concentration was increased from 30 ppm to 90 ppm, the photocatalytic efficiency decreased slightly from 98.9 % to 92 %. Thus, with high dye concentration, it reduces the transmission and path of photons and reduces the speed of light penetration into the dye solution.

From the survey results of affecting factors: reactions in room temperature of 50mg CQDs/MIL-101(Cr) photocatalyst with increasing dye concentration from 30 ppm to 90 ppm, were used to investigate the kinetics of RR195 photodegradation. The assumption that the reaction is first-order was established based on the equation:

$$-\ln\left(\frac{C_t}{C_o}\right) = k_p.t$$

In which C_t and C_o are the concentration of the dye at time t and initial time (t=0), k_p is the first-order rate constant.

The RR195 degradation on CQDs/MIL–101(Cr) photocatalysts followed first-order kinetics with equations 30ppm: y=1.6645+0.532x (R^2=0.985); 50 ppm: y=1.622 + 0.447x (R^2=0.994); 70ppm: y=1.441+0.436x (R^2=0.986) and 90ppm: y=0.8584+0.4103 (R^2= 0.994) respectively. MIL-101(Cr), with the advantages of surface area and pore size, helps to adsorb RR195 to the active phase surface. Then, when irradiating a sufficient solar light source, electrons on CQDs will separate from valance band to the conduction band, generating e-/h+ pairs. Under the irradiating of relevant wavelength, electrons and holes transfer to the material surface and interact with some absorbed substances such as water and oxygen to create free radicals on the semiconductor surface like ·OH and ·O2-. These free radicals are the main decomposing agents of organic compounds. The reactions take place in the RR195 photocatalytic process using CQDs/MIL-101(Cr) catalyst are described as follow:

CQDs/MIL-101(Cr) + sunlight irradation → $e_{cb}^- + h_{vb}^+$

$$e_{cb}^- + O_2 \rightarrow \cdot O_2^-$$
$$h_{vb}^+ + H_2O \rightarrow OH\cdot$$
$$H_2O_2 + e^- \rightarrow \cdot OH + OH^-$$
$$\cdot O_2^- + RR195 \rightarrow \text{degradation products}$$
$$\cdot OH + RR195 \rightarrow \text{degradation products}$$

4. Conclusion

This research, we successfully synthesized MIL-101(Cr) from terephthalic acid by hydrothermal method at 220°C for 9h and CQDs material from chitosan by hydrothermal method at 180°C for 12h. Then, CQDs/MIL-101(Cr) was synthesized by the synthesis of CQDs formation on the surface of and MIL-101(Cr). CQDs/MIL-101(Cr) expressed high photocatalytic character in degradation RR195 dye. Especially, 50% CQDs/MIL-101(Cr) catalyst samples showed a high dye degradation efficiency of 96% and investigated the influence of factors: 50 mg CQDs/MIL-101(Cr), dye concentration: 50 ppm, reaction time: 4h, a 300 W Xenon lamp.

Acknowledgements

This research is funded by Vietnam Maritime University under grant number: DT23-24.124

References

1. Pardeep Singh, Anwesha Borthakur, P.K Mishra, Dhanesh Tiwary, 2019.
2. Łukasz Janus, Marek Pia˛tkowski, Julia Radwan-Pragłowska, Dariusz Bogdał and Dalibor Matysek, Nanomaterials (2019). https://doi.org/10.3390/nano9020274.
3. Rongbin Lin, Shumin Li, Jingyun Wang, Jiapeng Xu, Chunhui Xu, Jin Wang, Chunxia Li and Zhengquan Li, Inorganic chemistry (2019). https:/doi.org/10.1039/C8QI01164H.
4. Xiaoyan Wei, Yawen Wang, Yu Huang, Caimei Fan, Journal of Alloys and Compounds 802 (2019) 467-476. https://doi.org/10.1016/j.jallcom.2019.06.086.
5. Jianwei Ren, Xoliswa Dyosiba, Nicholas M. Musyoka, Henrietta W. Langmi, Brian C. North, Mkhulu Mathe, Marice S. Onyango, International Journal of Hydrogen energy 41 (2016) 18141-18146. https://doi.org/10.1016/J.IJHYDENE.2016.08.040.
6. X.N. Pham, V.T. Vu, H.V.T. Nguyen, T.T.B. Nguyen, H. V. Doan, Nanoscale Advances. 4 (2022) 3600–3608. https://doi.org/10.1039/d2na00371f.
7. X. Zhou, W. Huang, J. Shi, Z. Zhao, q. Xia, Y. Li, H. Wang and Z. Li, J, Mater. Chem. A 2(13) (2014) 4722–4730.
8. D. Yin, C. Li, H. Ren, O. Shekhah, J. Liu, and C. Liang, RSC Advances 7 (3) (2017). https://doi.org/10.1039/c6ra25722d.
9. Z. Li, G. Che, W. Jiang, L. Liu, and H. Wang, RSC Advances 9 (7) (2019) 57. https://doi.org/10.1039/c9ra05600a.
10. Patrick S.Bárcia, Daniela Guimarães , Patrícia A.P. Mendes, José A.C. Silva, Vincent Guillermc, Hubert Chevreau, Christian Serre, Alírio E. Rodrigues, Micropor. Mesopor. Mat. 139 (2011) 67–73. https://doi.org/10.1016/j.micromeso.2010.10.019.
11. S. Ahmed, M. G. Rasul, W. N. Martens, R. Brown, and M. A. Hashib, Desalination 261 (1–2) (2010). https://doi.org/10.1016/j.desal.2010.04.06